Annals of Botany **114**: 513–524, 2014
doi:10.1093/aob/mcu128, available online at www.aob.oxfordjournals.org

ANNALS OF BOTANY
Founded 1887

Explaining ontogenetic shifts in root–shoot scaling with transient dynamics

Théophile Lohier[1], Franck Jabot[1,*], Driss Meziane[2], Bill Shipley[3], Peter B. Reich[4,5] and Guillaume Deffuant[1]

[1]*LISC – Laboratoire d'Ingénierie pour les Systèmes complexes, IRSTEA, 9 avenue Blaise Pascal, CS 20085, 63178 Aubière, France,* [2]*Université Sidi Mohamed Ben Abdellah, Faculté des sciences Dhrar El Mehraz, Département de biologie, BP 1796, Fès, Atlas, Morocco,* [3]*Département de biologie, Université de Sherbrooke, Sherbrooke (Qc), J1K 2R1, Canada,* [4]*Department of Forest Resources, University of Minnesota, St. Paul MN 55108, USA and* [5]*Hawkesbury Institute for the Environment, University of Western Sidney, Locked Bag 1797, Penrith, NSW 2751, Australia*
** For correspondence. E-mail franck.jabot@irstea.fr*

Received: 25 October 2013 Returned for revision: 2 December 2013 Accepted: 12 May 2014 Published electronically: 2 July 2014

• **Background and Aims** Simple models of herbaceous plant growth based on optimal partitioning theory predict, at steady state, an isometric relationship between shoot and root biomass during plant ontogeny, i.e. a constant root–shoot ratio. This prediction has received mixed empirical support, suggesting either that optimal partitioning is too coarse an assumption to model plant biomass allocation, or that additional processes need to be modelled to account for empirical findings within the optimal partitioning framework. In this study, simulations are used to compare quantitatively two potential explanations for observed non-isometric relationships, namely nutrient limitation during the experiments and initial developmental constraints.
• **Methods** A simple plant growth model was built to simulate the growth of herbaceous species, based on optimal partitioning theory combined with empirically measured plant functional traits. Its ability to reproduce plant relative growth rate and final root weight ratio was assessed against previously published data. Predicted root–shoot ratios during plant ontogeny were compared with experimental observations. The effects of nutrient limitation and initial developmental constraints on root–shoot ratios were then tested.
• **Key Results** The model was found to reproduce overall plant growth patterns accurately, but failed, in its simplest form, at explaining non-isometric growth trajectories. Both nutrient limitation and ontogenetic developmental constraints were further shown to cause transient dynamics resulting in a deviation from isometry. Nitrogen limitation alone was not sufficient to explain the observed trajectories of most plant species. The inclusion of initial developmental constraints (fixed non-optimal initial root–shoot ratios) enabled the reproduction of the observed trajectories and were consistent with observed initial root–shoot ratios.
• **Conclusions** This study highlights the fact that considering transient dynamics enables theoretical predictions based on optimal partitioning to be reconciled with empirically measured ontogenetic root–shoot allometries. The transient dynamics cannot be solely explained by nutrient limitation during the experiments, pointing to a likely role for initial developmental constraints in the observed non-isometric growth trajectories.

Key words: Allometry, biomass partitioning, functional trait, grassland, plant growth model, model selection, ontogenetic shift, optimal partitioning theory, root–shoot ratio, transient dynamics.

INTRODUCTION

Plants both fix atmospheric carbon in their leaves by photosynthesis and capture soil water and nutrients by their roots. The way in which these basic resources are allocated among different plant organs during plant growth is of utmost importance to understanding such basic ecological phenomena as competition between plants (Tilman, 1988; Grime, 2001), the global carbon cycle and the consequences of rising atmospheric carbon dioxide (Hungate *et al*., 1997; Mokany *et al*., 2006; Bonan, 2008). Allocation of biomass between roots and shoots in plants has received much attention (Poorter *et al*., 2012). This allocation strongly depends on environmental conditions (Chapin, 1980; Poorter *et al*., 2012), so that it constitutes a major difficulty for plant growth modelling (Thornley, 1995; Le Roux *et al*., 2001).

Many approaches have been used to model allocation in plants (Génard *et al*., 2008; Franklin *et al*., 2012). Allometric relationships (Niklas, 1994; West *et al*., 1999) can be used to constrain the growth of different plant parts so that allometric equations are always satisfied during plant ontogeny (Taubert *et al*., 2012). Although this approach is conceptually and technically simple, it requires empirical measurements of allometric coefficients in multiple environmental conditions. As a result, this approach cannot predict how allometric relationships are likely to vary depending on the environmental conditions encountered by the plant (Bloom *et al*., 1985). A second approach is to represent the capture of basic resources by the plant and their transport across different plant organs (Thornley, 1998). This approach aims at being mechanistic, but it requires the quantification of mechanistic properties such as the resistance to nutrient flow in the plant, as well as processes of internal regulation. A third type of approach relies on various optimization principles. Studies of this type generally consider that allocation in the plant aims at maximizing some criterion, used as a proxy for plant fitness, such as plant relative growth rate (RGR; Charles-Edwards *et al*., 1972; Reynolds and Chen, 1996).

They sometimes also make use of game-theoretic or adaptive dynamics methods to take into account the ecological and evolutionary impacts of competition between plants (Franklin *et al*., 2012; McNickle and Dybzinski, 2013).

The idea that plants may allocate their assimilates among organs so as to balance their root activity of water and nutrient uptake and their shoot activity of photosynthesis dates back at least to the work of Brouwer (1962). Since then, this hypothesis has been variously called 'optimal partitioning', 'functional equilibrium' or the 'balanced growth hypothesis' (Poorter *et al*., 2012). This simple idea has proven powerful at qualitatively explaining how environmental conditions and perturbations affect patterns of root–shoot allocation (Iwasa and Roughgarden, 1984; Bloom *et al*., 1985; Poorter *et al*., 2012). Optimal partitioning is thus used in a large number of plant growth models (Shipley and Meziane, 2002; Franklin *et al*., 2012).

Some simple models of plant growth that assume optimal partitioning predict an isometric relationship between shoot and root biomass during the exponential phase of growth in non-limiting conditions, i.e. root and shoot biomass remain proportional (Charles-Edwards, 1976; Robinson, 1986; Shipley and Meziane, 2002). This prediction has received mixed empirical support. According to the meta-analysis of Poorter *et al*. (2012), ontogenetic shifts in root–shoot ratios are variable across experiments performed so far. For instance, McConnaughay and Coleman (1999) explored the impact of resource gradients on three annual species and found that the root–shoot ratio decreases during plant development. Müller *et al*. (2000) studied allocation patterns of 27 herbaceous plant species and also found a decreasing root–shoot ratio for 14 species. In contrast, Shipley and Meziane (2002) studied 22 herbaceous plant species during 35 d and found a preferential allocation to roots during plant ontogeny in general, although deviations from isometry were weak in most cases. Arredondo *et al*. (1998) also found an increase in the root–shoot ratio during plant ontogeny. The variable root–shoot ratios evidenced in these studies question the validity of the optimal partitioning hypothesis.

However, rather than a fundamental flaw in the assumption of optimal partitioning, the discrepancies between data and model predictions could also be due to the requirement for additional model assumptions beyond optimal partitioning. For instance, Reynolds and Thornley (1982), Johnson (1985) and Johnson and Thornley (1987) made the point that optimal partitioning implied that plants should be equally limited by shoot and root activities, which do not need to be constant over time, but rather depend on dynamic environmental conditions and potential disturbances. In this vein, Shipley and Meziane (2002) argued that non-isometric relationships may be explained by a progressive nitrogen limitation of plant growth during experiments or by a decrease of intrinsic root uptake capacity with age. These two features are susceptible to causing a transient phase of preferential allocation to roots (Ingestad and Ågren, 1991). An alternative explanation for non-isometric trajectories might be that root–shoot partitioning is ontogenetically constrained, especially during the early stages of growth (Gedroc *et al*., 1996). If allocation is ontogenetically constrained, the shoot–root ratio is likely to differ from the ratio predicted by optimal partitioning. Importantly, even if developmental constraints cease early during plant ontogeny, they are likely to have persistent effects on plant growth trajectories during a transient phase of root–shoot ratio adjustment by the plant. This will be tested here by considering that the initial shoot–root ratio may differ from that predicted by optimal partitioning, but that subsequent dynamics are controlled by optimal partitioning equations. Transient dynamics, due either to nutrient limitation or to some initial developmental constraints, could potentially explain the discrepancy between steady-state predictions based on optimal partitioning theory and experimental findings. This study aims at quantitatively testing these potential explanations.

The study is structured in three main parts. First, a simple plant growth model is built, which is based on the optimal partitioning hypothesis and on plant functional traits that can be empirically measured in practice. This model represents the basic processes of photosynthesis, nutrient uptake, and root–shoot carbon and nitrogen allocation. Secondly, we investigate the ability of such a simple model to reproduce patterns of RGR and final root weight ratio (RWR) experimentally measured for 25 species by Reich *et al*. (2003). This particular study was chosen because most plant traits used in the model were measured during the experiments. The other model parameters, which were not experimentally measured, are estimated so as to maximize the model fit to the two growth indicators (RGR and RWR). Model goodness of fit is then assessed, as well as the realism of fitted parameter values. This part of the study served to determine if the simple model considered is a realistic approximation of plant growth dynamics. Thirdly, armed with this simple but realistic plant growth model, the experiments of Shipley and Meziane (2002) are re-analysed. In these experiments, root and shoot biomass trajectories of 22 plant species were measured experimentally in varying environmental conditions. The simple model is shown not to be able to explain the observed non-isometric root–shoot biomass relationships when model parameters are constrained so that the model accurately fits overall plant growth data. We then test whether adding nitrogen limitation and a decrease of root uptake capacity with root age may lead to the observed non-isometric relationships. We finally explore whether considering ontogenetic constraints through variations in the initial shoot–root ratio may improve the model fit to data. Fitted initial shoot–root ratios were finally compared with observed ratios by re-analysing the data of Shipley and Meziane (2002).

MODEL DESCRIPTION

The model simulates the growth of herbaceous species in non-limiting conditions of water supply. In this model, a plant is described by its total biomass $B(t)$ at time t. This biomass is divided into above- (B_s) and below- (B_r) ground biomass, so that:

$$B(t) = B_s(t) + B_r(t) \quad (1)$$

Four growth processes are modelled: (1) shoot photosynthesis; (2) nitrogen uptake by roots; (3) nitrogen allocation among roots and shoots; and (4) carbon allocation among roots and shoots. Leaves and stems are not distinguished in the shoot component for two reasons. First, since both leaves and stems contribute to photosynthesis in herbaceous plants (Nilsen, 1995), pooling these two plant components makes sense functionally. Secondly, distinguishing these two plant components would

increase model complexity by adding leaf- and stem-specific activity rates (photosynthesis and respiration) and two additional leaf–stem allocation rules for carbon and nitrogen, while these processes are poorly documented. Certainly, increasing the complexity of the model with both stem and leaf components could be easily achieved for cases in which additional information is available.

Plant development

A simple difference equation is used with one time step representing 1 h. The plant biomass at $t + 1$ is given by:

$$B(t+1) = B(t) + \Delta B(t) = B(t) + P_{net}(t) \quad (2)$$

where $P_{net}(t)$ is the net primary production at time t.

The increases of shoot and root biomass between times t and $t + 1$ are described by eqns (3) and (4) respectively:

$$\Delta B_s(t) = a(t) \times P_{net}(t) \quad (3)$$

$$\Delta B_r(t) = [1 - a(t)] \times P_{net}(t) \quad (4)$$

where $a(t)$ is the portion of net primary production allocated to shoot. The computations of $P_{net}(t)$ and $a(t)$ are detailed below.

Photosynthesis

Grasses perform photosynthesis in both their leaves and stems (Aschan and Pfanz, 2003). Although the stem photosynthetic rate may differ from the leaf photosynthetic rate, as well as mass–surface ratios, it will be assumed here for simplicity that these quantities are equal among stems and leaves and thus that net primary production $P_{net}(t)$ can be modelled by:

$$P_{net}(t) = C \times A_N(t) \times SLA \times B_s(t) - R_r \times B_r \quad (5)$$

where $A_N(t)$ is the leaf net photosynthetic rate expressed per unit leaf area, SLA is the specific leaf area, $B_s(t)$ is the shoot biomass, R_r is the root respiration rate, B_r is the root biomass and C is a constant accounting for the conversion of assimilated CO_2 into dry matter content. C is calculated from the stochiometry of photosynthetic reactions: to synthesize 1 mol of glucose ($C_6H_{12}O_6$) weighting 180 g, 6 mol of carbon dioxide (CO_2) are needed, hence $C = 180/6 = 30$ (Kikuzawa and Lechowicz, 2006). Equation (5) has been frequently used in plant growth modelling (see for instance Foley, 2007). Note that this approach is still valid if less strong assumptions are used, namely that the stem–leaf ratio is constant during plant ontogeny and that the stem photosynthetic rate responds to light conditions and plant nitrogen status similarly to leaf photosynthetic rate. In this case, $A_N(t)$ should be understood as an effective shoot net photosynthetic rate.

Net photosynthetic rate $A_N(t)$ has been shown to be linearly related to the nitrogen content of the shoot (Lambers *et al.*, 1998). Following Konings *et al.* (1989), the following relationship is used:

$$A_N(t) = [A_{max}(t)/LNC_{max}] \times [N_s(t)/B_s(t)] \quad (6)$$

where LNC_{max} is the leaf nitrogen content that maximizes photosynthesis, $N_s(t)$ is the nitrogen content of the shoot and $A_{max}(t)$ is the net maximal leaf photosynthetic rate in given light conditions:

$$A_{max}(t) = A_{sat} \times f[I_r(t)] - R_s \quad (7)$$

where A_{sat} is the light-saturated gross photosynthetic rate, R_s is the shoot respiration rate, $I_r(t)$ is the incoming irradiance at time t and $f(I_r)$ is a function varying between zero when I_r is null and one when it is optimal. This function accounts for the impact of ambient light on photosynthesis. In the following, the irradiance is assumed to be constant during the photoperiod and therefore $A_{max}(t)$ is also constant. Overnight the irradiance I_r is null, so f is null and $A_{max}(t)$ equals shoot respiration (R_s). As we are interested in the first stages of plant growth, the decrease of the net photosynthetic rate caused by self-shading and the resulting variations in root–shoot scaling are likely to be negligible and so self-shading will be ignored in the following.

Nitrogen uptake

When nutrient supply is non-limiting, nitrogen uptake is only limited by plant physiology and root biomass. So at time t, a plant is able to absorb at most:

$$N_p = U_{max} \times B_r(t) \quad (8)$$

where U_{max} is the mass-based root effective uptake capacity.

Roots are assumed to be able to adjust nitrogen uptake so as to match the nitrogen demand of the plant N_d (Schippers and Kropff, 2001). The latter corresponds to the amount of nitrogen required for the leaf content of new leaf biomass to be equal to LNC_{max}. N_d is thus given by:

$$N_d = [LNC_{max} \times \Delta B_s(t)]/a_N(t) \quad (9)$$

where $\Delta B_s(t)$ is the shoot biomass produced between t and $t + 1$, and $a_N(t)$ is the fraction of nitrogen captured between t and $t + 1$ which is allocated to shoot. Thereafter, assimilated nitrogen N_u equals the minimum of N_p and N_d:

$$N_u(t) = \min[N_p(t), N_d(t)] \quad (10)$$

Nitrogen allocation

Following Dybzinski *et al.* (2011), it is assumed that a fixed fraction of assimilated nitrogen is allocated to the shoot: $a_N(t) = a_N$. An alternative way for modelling nitrogen partitioning would be to use optimal partitioning theory (Mäkelä *et al.*, 2008). However, to apply this theory, it would be necessary to know the relationship between root uptake efficiency and root nitrogen content or to make some assumptions on the relationship between shoot and root nitrogen content (Mäkelä *et al.*, 2008; Valentine and Mäkelä, 2012).

Carbon allocation

An optimal allocation model is used for carbon allocation (Dewar *et al.*, 2009), in which plants are assumed to allocate assimilates so as to maximize their RGR. Assuming that

biomass and leaf nitrogen content at time t are known, we look for an allocation to shoot $a(t)$ such that RGR$(t+1)$ is maximal. RGR$(t+1)$ is given by:

$$\begin{aligned}\mathrm{RGR}(t+1) &= \Delta B(t+1)/B(t+1)\\ &= P_{\mathrm{net}}(t+1)/B(t+1)\end{aligned} \quad (11)$$

From eqns (5) and (6), RGR$(t+1)$ maximization is equivalent to maximize:

$$\begin{aligned}C \times [A_{\max}(t+1)/\mathrm{LNC}_{\max}] \times [N_{\mathrm{s}}(t+1)/B_{\mathrm{s}}(t+1)]\\ \times \mathrm{SLA} \times B_{\mathrm{s}}(t+1) - R_{\mathrm{r}} \times B_{\mathrm{r}}\end{aligned} \quad (12)$$

Given that:

$$N_{\mathrm{s}}(t+1) = N_{\mathrm{s}}(t) + N_{\mathrm{u}}(t) \quad (13)$$

RGR$(t+1)$ is maximal when $N_{\mathrm{u}}(t)$ is maximal. In other words, RGR$(t+1)$ is maximal when the nitrogen demand at t + 1 is equal to the potential uptake $N_{\mathrm{p}}(t)$:

$$\mathrm{LNC}_{\max} \times a(t) \times P_{\mathrm{net}}(t) = N_{\mathrm{p}}(t) \quad (14)$$

Hence the shoot allocation factor $a(t)$ is given by:

$$a(t) = N_{\mathrm{p}}(t)/[\mathrm{LNC}_{\max} \times P_{\mathrm{net}}(t)] \quad (15)$$

In summary, the model takes as input seven parameters ($A_{\max}$, R_{s}, R_{r}, $\mathrm{LNC}_{\max}$, SLA, $U_{\max}$ and a_{N}). Most of the parameters are commonly measured plant functional traits (Kattge *et al.*, 2011). $A_{\max}$, R_{s}, R_{r}, $\mathrm{LNC}_{\max}$ and SLA were measured in the experiments of Reich *et al.* (2003), and $\mathrm{LNC}_{\max}$ and SLA in the experiments of Meziane and Shipley (1999). Note that plant senescence was neglected, since we are interested here in the first stages of plant development.

PARAMETER ESTIMATION AND MODEL SELECTION

In this section, the data set used to test the model ability to reproduce real plant growth dynamics is first presented. The fitting procedure of the remaining unmeasured model parameters is then detailed. The results of this model–data comparison procedure are presented in the last sub-section.

Plant growth data

An experiment performed by Reich *et al.* (2003) is used, in which 34 herbaceous and woody plant species were grown in monoculture under controlled environmental glasshouse conditions, for 9 weeks after germination. Herein we use 25 of these species (just the herbaceous non-leguminous ones), growing under fertilized conditions (ignoring ambient grown plant) to minimize N limitations. Beginning 2 weeks after sowing, pots received 30 mL of half-strength Hoagland's solution three times per week. Pots were watered as needed between treatment applications to maintain soils near field capacity. Supplemental lighting provided an additional 130–170 μmol $\mathrm{m}^{-2}\mathrm{s}^{-1}$ above ambient light levels during a 14 h photoperiod. Each 3 weeks, plants were harvested and the biomass of the different plant components (leaves, stem and roots) were measured. From these measurements, several quantities were computed: the RWR equal to the root biomass divided by the total plant biomass; and the RGR computed as in Evans (1972):

$$\mathrm{RGR} = \{\ln[B(t_2)] - \ln[B(t_1)]\}/(t_2 - t_1) \quad (16)$$

where t_1 and t_2 are harvesting dates.

Several plant functional traits were also measured: the light-saturated photosynthetic rate A_{sat}, the shoot and root respiration rate R_{s} and R_{r}, the leaf nitrogen content LNC, the root nitrogen content RNC and the specific leaf area SLA. RNC is not a model parameter, but it enables the nitrogen allocation coefficient a_{N} to be computed with the following equation:

$$\begin{aligned}a_{\mathrm{N}} = [N_{\mathrm{s}}(t_{\mathrm{end}})/B_{\mathrm{s}}(t_{\mathrm{end}})]/\{[N_{\mathrm{s}}(t_{\mathrm{end}})/B_{\mathrm{s}}(t_{\mathrm{end}})] + \mathrm{RNC}\\ \times [B_{\mathrm{r}}(t_{\mathrm{end}})/B_{\mathrm{s}}(t_{\mathrm{end}})]\}\end{aligned} \quad (17)$$

This data set enables us to assess the model's ability to explain observed plant growth patterns, when it is strongly constrained by empirically measured plant traits.

Fitting the model on experimental data

Following Goudriaan and Van Laar (1994), the initial shoot–root ratio was set to 1. Initial root and shoot biomass values do not affect the computed growth indicator, so they are arbitrarily set to 0·5 mg. The maximal nutrient uptake efficiency $U_{\max}$ was not measured in the experiments of Reich *et al.* (2003) and thus had to be estimated. Besides, the maximal photosynthetic efficiency $A_{\max}$ was measured for an irradiance of 1000 μmol $\mathrm{m}^{-2}\,\mathrm{s}^{-1}$, while plants were not grown under constant light conditions. The effective $A_{\max}$ during the experiments, resulting from the variable light conditions, was therefore estimated. These two parameters were estimated by fitting the plant growth model to the growth data of the experiments of Reich *et al.* (2003). A distance ε between model predictions and experimental data was defined. It was based on two experimentally measured growth indicators: the plant RGR and final RWR. ε was defined as:

$$\varepsilon = \sqrt{\frac{1}{2} \times \frac{\sum_{i=1}^{2} (X_{i,\mathrm{obs}} - X_{i,\mathrm{sim}})^2}{(X_{i,\mathrm{obs}})^2}} \quad (18)$$

where $X_{\mathrm{sim}} = (\mathrm{RGR}_{\mathrm{sim}}, \mathrm{RWR}_{\mathrm{sim}})$ and $X_{\mathrm{obs}} = (\mathrm{RGR}_{\mathrm{obs}}, \mathrm{RWR}_{\mathrm{obs}})$ are the growth indicators of the simulations and of the experimental data, respectively.

This distance ε was computed on a 50 × 190 grid of parameter values described in Table 1, and the parameter set that minimized this distance was retained. The parameter space was chosen so as to include the reported parameter values found in the literature (Table 1). Note that the interval chosen for $A_{\max}$ does not include the largest values measured by Reich *et al.* (2003). In this experiment, the photosynthetic efficiency was measured in optimal light conditions [$f(I_{\mathrm{r}}) = 1$]. However, plants were not grown in optimal light conditions, so that the effective photosynthetic efficiency is necessarily smaller than the light-saturated photosynthetic efficiency.

TABLE 1. *Parameter ranges reported in the literature and those used for model calibration with the experiments of Reich et al. (2003)*

	A_{max} (nmol g^{-1} s^{-1})	U_{max} (mg g^{-1} h^{-1})
Range reported in the literature	150–900*	0·22–0·92†
Range used for model calibration	100–600	0·10–2·00
Grid step used for model calibration	10	0·01

*Reich *et al.* (2003).
†Maire *et al.* (2009).

TABLE 2. *Average estimates of model parameters and associated minimal distance between model predictions and empirical data*

Species	A_{max} (nmol g^{-1} s^{-1})	U_{max} (mg g^{-1} h^{-1})	ε_{min} (%)
Achillea millefolium (AcM)	262 (9·85)	0·87 (0·064)	0·6
Anemone cylindrica (AnC)	184 (5·06)	0·75 (0·048)	1·4
Asclepias tuberosa (AsT)	200 (7·62)	0·55 (0·039)	0·2
Aster azureus (AsA)	282 (9·37)	1·64 (0·104)	0·8
Coreopsis palmata (CoP)	269 (7·93)	0·90 (0·058)	0·0
Liatris aspera (LiA)	154 (4·99)	1·29 (0·063)	3·0
Monarda fistulosa (MoF)	259 (7·93)	0·85 (0·062)	0·3
Rudbeckia hirta (RuH)	261 (9·85)	0·73 (0·056)	0·3
Solidago nemoralis (SoN)	–	–	11·2
Agropyron repens (AgR)	183 (4·83)	0·55 (0·038)	0·8
Agropyron smithii (AgS)	170 (0·00)	0·59 (0·045)	0·6
Bromus inermis (BrI)	228 (11·38)	0·31 (0·031)	0·8
Calamagrostis canadensis (CaC)	217 (7·35)	0·77 (0·051)	0·8
Elymus canadensis (ElC)	191 (7·03)	0·55 (0·039)	0·7
Koeleria cristata (KoC)	259 (7·73)	1·06 (0·068)	0·2
Leersia oryzoides (LeO)	291 (7·72)	0·64 (0·040)	1·0
Stipa comata (StC)	153 (4·89)	0·49 (0·035)	1·4
Andropogon gerardii (AnG)	215 (5·11)	0·49 (0·037)	1·7
Bouteloua curtipendula (BoC)	229 (7·55)	0·80 (0·050)	0·6
Bouteloua gracilis (BoG)	180 (0·00)	1·17 (0·079)	0·0
Buchloe dactyloides (BuD)	240 (7·84)	0·44 (0·034)	0·3
Panicum vigatum (PaV)	194 (5·08)	0·68 (0·043)	2·1
Schyzarchyrium scoparium (ScC)	184 (5·06)	0·76 (0·046)	2·3
Sorghastrums nutans (SoNb)	224 (5·03)	0·50 (0·033)	1·0
Sporobolus cryptandrus (SpC)	213 (4·71)	1·17 (0·066)	0·8

Empirical growth indicators have been measured with observation errors of 5–10 % (Reich *et al.*, 2003). Therefore, all sets of parameters leading to ε values <0·05 are retained. They form an interval of likely values for A_{max} and U_{max}, which were relatively narrow (Table 2).

Results

The coefficients of variation of the two model parameters A_{max} and U_{max} were <5 and 10 %, respectively (Table 2), which means that the growth data used were sufficiently informative to obtain accurate parameter estimates of the minimal version of the model. Model parameter estimates are realistic compared with the range of values reported in the literature (Table 1). Importantly, the remaining lack of fit of the model to data, leading to a residual error ε_{min} (Table 2), was negligible compared with the observed interspecific variations of growth indicators [Fig. 1, average normalized root mean square error (NRMSE) = 3·47 %]. This means that this simple trait-based model was sufficient to capture interspecific differences in growth rates as well as in root–shoot carbon and nitrogen partitioning.

The growth dynamics predicted by the fitted minimal version of the model consist of a short transient phase during which carbon allocation $a(t)$ varies, followed by a steady-state regime of exponential growth during which carbon allocation is constant (Fig. 2A) and root and shoot growth rates scale proportionally (Fig. 2B), leading to an allometric coefficient β equal to 1 (Fig. 2C). The predicted duration of the transient phase depends on the species identity, but never exceeds 15 d (Fig. 2C). In the 35 d experiments of Shipley and Meziane (2002), the first measurements occurred 15 d after germination (shown by the dashed lines in Fig. 2B, C). Therefore, the duration of transient dynamics in the minimal version of the model is insufficient to explain the observed deviations from isometry observed in the 35 d experiments of Shipley and Meziane (2002). These authors suggested that the observed deviation from isometry could come from a progressive appearance of nitrogen limitation in the experimental setting in which nitrogen was added in fixed amounts. They also discussed that a decrease of intrinsic root uptake capacity with root age could contribute to non-isometric growth trajectories. These two additional processes were included in the model to assess their ability to explain observed patterns. It has been further assessed whether a modification of the initial (ontogenetically constrained) shoot–root ratio could significantly contribute to the observed non-isometric trajectories.

ALLOMETRIC PREDICTIONS

In this section, the data set used to test the model predictions on root–shoot allometry is first presented. Two additional model ingredients are then introduced: (1) the consideration of nitrogen consumption during the experiment potentially causing some nitrogen limitation for plants, especially at the end of the experiment; and (2) the inclusion of a decrease in root uptake capacity as they age. The impact of the initial shoot–root ratio on allometric patterns was also investigated. Thirdly, the model–data fitting procedure was detailed, as well as the associated test of whether the different models studied are able to reproduce the empirical root–shoot allometries. Fourthly, the results of this model–data comparison procedure are presented.

Plant growth data

Given that Reich *et al.* (2003) did not perform detailed measures of allometric relationships (they only performed three sequential harvests), a second data set collected by Meziane and Shipley (1999) and Shipley and Meziane (2002) is used. In this experiment, a total of 1150 plants from 22 different herbaceous plant species were grown in hydroponic sand monoculture in factorial combinations of high [1100 μmol $m^{-2}s^{-1}$ photosynthetically active radiation (PAR)] and low (200 μmol m^{-2} s^{-1} PAR) irradiance crossed with a full-strength and a 1/6 dilution of Hoagland's hydroponic solution. Each plant grew in a separate 1·3 dm^3 container in a growth chamber with 15/9 h light:dark cycles. Each plant grew in one of four resource environments: high (L, 1100 μmol m^{-2} s^{-1}) and low (l, μmol m^{-2} s^{-1}) irradiance combined with high (N, full-strength Hoagland's nutrient solution) and low (n, 1/6 dilution) external nutrient concentrations.

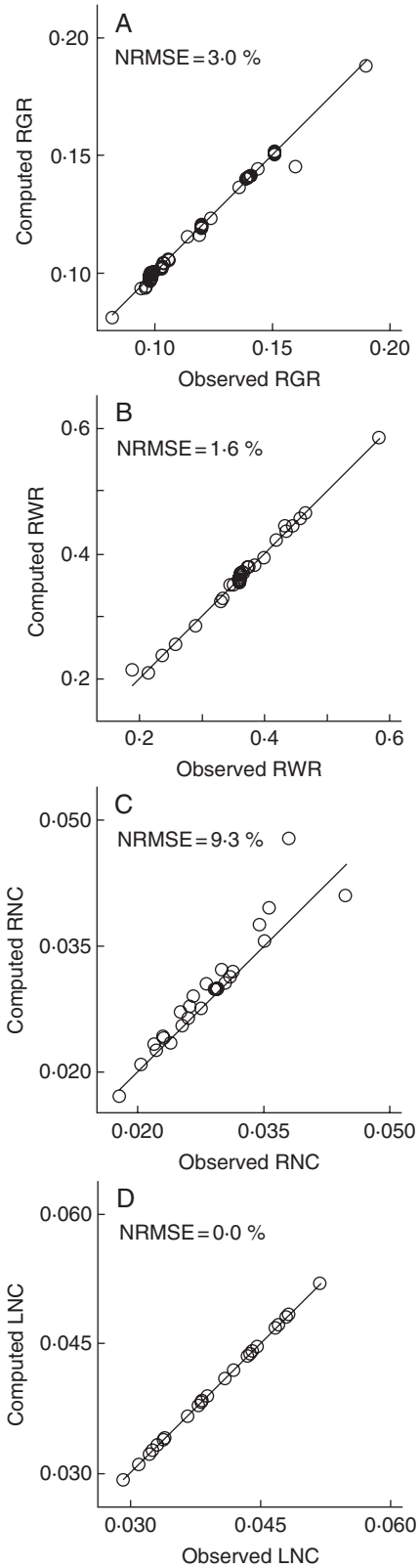

FIG. 1. (A) Computed relative growth rates (RGRs) against measured RGRs. (B) Computed root weight ratios (RWRs) against measured RWRs. (C) Computed root nitrogen contents (RNCs) against measured RNCs. (D) Computed leaf nitrogen contents (LNCs) against measured LNCs. The solid line represents $y = x$. Each circle represents a plant species. NRMSE, normalized root mean square error.

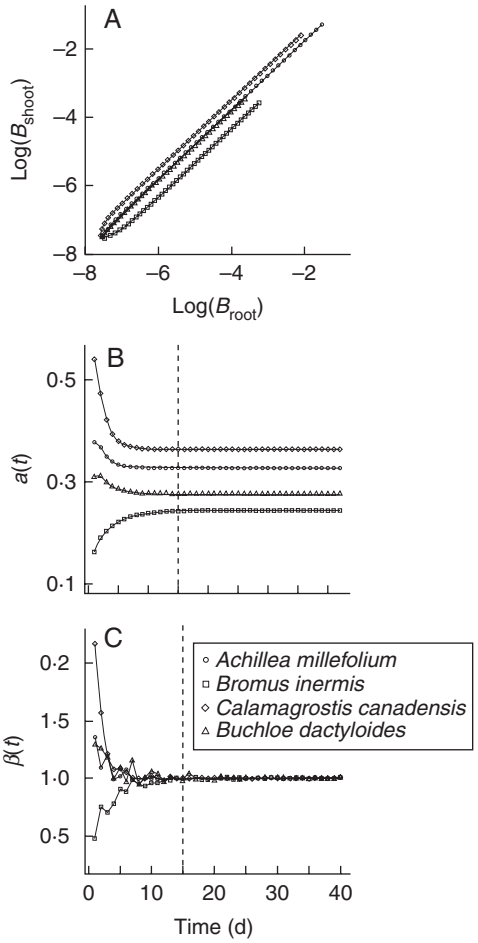

FIG. 2. (A) Bivariate plots of shoot and root simulated dynamics. (B) Simulated dynamics of the carbon fraction allocated to above-ground biomass. (C) Simulated dynamics of the allometric coefficient β. Each symbol stands for a particular species, as indicated in the key in (C). Best-fit parameters were used in the simulations of the minimal model. The first harvest in the experiment of Shipley and Meziane (2002) is shown by a vertical dashed line.

These four experimental treatments are termed LN, Ln, lN and ln treatments, respectively. Each container was filled to field capacity with the nutrient solution three times a day. Plants were harvested and the biomass of leaves, stems and roots was measured at 15, 20, 25, 30 and 35 d post-germination. Two plant functional traits were measured: LNC and SLA. RWR was computed, as well as average RGR, computed as the slope of a regression of the natural logarithm of plant dry mass on the harvest date. Allometric relationships between shoot and root biomass during plant ontogeny was further measured, using an equation of the form:

$$B_s = \alpha \times B_r^{\beta} \tag{19}$$

which can be rewritten as:

$$\ln(B_s) = \ln(\alpha) + \beta \times \ln(B_r) \tag{20}$$

The allometric coefficient β was thus computed as the slope of a regression of the natural logarithm of shoot dry mass on the natural logarithm of root dry mass. This second data set was

not used for model checking, since fewer plant functional traits were measured empirically, and thus it would have been a less conservative test of the model with a larger number of unmeasured model parameters and a smaller number of growth indicators to match. Rather, it was used to confront the model predictions with empirically measured allometric data.

Adding nitrogen consumption by plants in the containers

Following Engels *et al.* (2000), Hane's relationship was used to model the dependency of uptake rate $U(t)$ on substrate concentration:

$$U(t) = U_{max} \times [N]_{soil}(t)/\{K_m + [N]_{soil}(t)\} \quad (21)$$

where K_m is the substrate affinity and $[N]_{soil}(t)$ is the nitrogen concentration in soil at time t. Initially soil nitrogen content equals:

$$N_{soil}(t_0) = [N]_{Hoagland} \times V \times C_{soil} \quad (22)$$

where $[N]_{Hoagland}$ is the nitrogen concentration in the hydroponic solution used in the experiment (0·210 g L^{-1} for full-strength solution, 1/6 of this value in the low nitrogen treatment), V is the container volume (1·3 L) and C_{soil} is the volumetric soil moisture content remaining at field capacity (approx. 5 % according to Tucker, 1999). Then soil nitrogen content is computed at each time step as:

$$N_{soil}(t) = N_{soil}(t-1) - N_u(t-1) \quad (23)$$

where $N_u(t)$ is the amount of nitrogen absorbed by the plant at time t [eqn (12)]. Every 8 h each container is filled to field capacity with the nutrient solution, so these dynamics of decrease in nitrogen concentration in the container are restarted.

Adding a decrease of root uptake capacity with root age

The model of decrease in root uptake efficiency as they age is based on the observations of Volder *et al.* (2005). Root biomass is divided into several layers. Each layer has its own biomass, age and nitrogen uptake capacity. At the beginning of each time step t, a root layer is added with a biomass corresponding to the newly produced root biomass $\Delta B_r(t-1)$. A root layer i will have a nitrogen uptake capacity varying with time $U_i(t)$ given by:

$$U_{max,i}(t) = U_{max} \times [1 + 2 \times e^{-\rho(t-t_i)}]/3 \quad (24)$$

where ρ is the decay rate of root nitrogen uptake efficiency, and t_i is the time of appearance of the root layer i. Following Volder *et al.* (2005), it is assumed that after some days root uptake efficiency stabilizes at around one-third of maximal efficiency.

Adding variation in initial root–shoot ratio

Since the first measurements in the experiment of Shipley and Meziane (2002) occurred 15 d after germination, no information is available on growth trajectories during the very first days of the experiment. Two hypotheses were compared regarding allocation patterns during these first 15 d. (H_0) Biomass is optimally allocated, so that the shoot–root ratio at first measurement, called the initial shoot–root ratio R_0 in the following, is the ratio required for optimal partitioning, R_{opt}. (H_1) Because of ontogenetic developmental constraints, the initial shoot–root ratio R_{ont} differs from the optimal one:

$$\left.\begin{aligned}(H_0) : B_s(t_0) &= R_{opt} \times B_r(t_0)\\ (H_1) : B_s(t_0) &= R_{ont} \times B_r(t_0)\end{aligned}\right\} \quad (25)$$

These additional model ingredients are used to build three models. The first one does not include nitrogen limitation and assumes that the initial shoot–root ratio corresponds to the ratio predicted by optimal partitioning (M_0). The second one additionally includes nitrogen consumption and decrease in root uptake capacity with age (M_1). The third one additionally authorizes initial shoot–root ratios differing from the optimal one (M_2). Each model was fitted to the same data of Shipley and Meziane (2002) which have been obtained in four resource environments: high and low irradiance combined with high and low external nitrogen concentration. Importantly, all modelled dynamics are based on optimal partitioning theory: in model M_2, developmental constraints cease after the first 15 d and only affect the initial conditions.

Fitting models to experimental data

Five parameters, the photosynthetic efficiency A_{max}, the shoot and root respiration rates R_s and R_r, the nitrogen allocation a_N and the maximal nutrient uptake efficiency U_{max}, were not measured in the experiments of Meziane and Shipley (1999). Average shoot and root respiration $R_{s,mean}$ and $R_{r,mean}$ were computed from the data of Reich *et al.* (2003), and the average values $R_{s,mean} = R_{r,mean} = 40$ nmol g^{-1} s^{-1} was used for all the species

TABLE 3. *Parameter ranges reported in the literature and those used for model calibration with the experiments of Shipley and Meziane (2002)*

	A_{max} (nmol g^{-1} s^{-1})	U_{max} (mg g^{-1} h^{-1})	a_N (%)	ρ (mg g^{-1} h^{-1})	K_m (mg L^{-1})	R_0
Range reported in the literature	150–900*	0·22–0·92†	50–70*	0·025‡	0·06–0·56§	1·0¶
Range used for model calibration	100–700	0·10–2·50	50–90	0·0–0·030	0·0–2·0	0·5–5·0
Grid step used for model calibration	25	0·10	10	0·005	0·25	0·25

*Reich *et al.* (2003).
†Maire *et al.* (2009).
‡Volder *et al.* (2005).
§Morris (1980).
¶Goudriaan and Van Laar (1994).

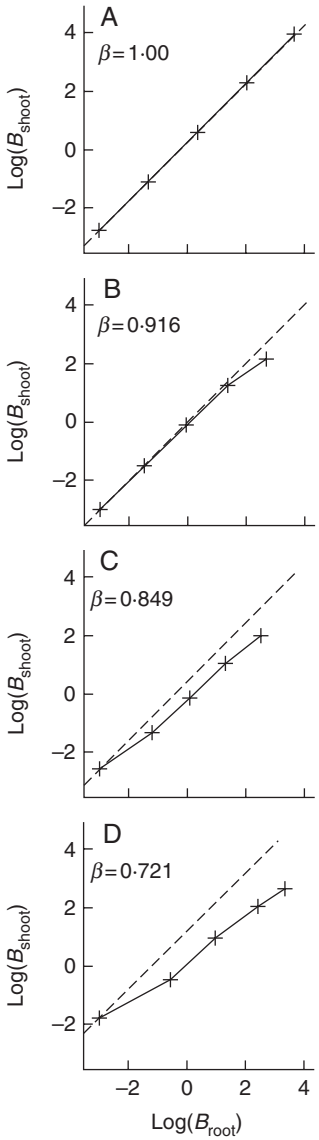

FIG. 3. Root–shoot trajectories of *Eupatorium maculatum* simulated with (A) the reference model M_0, (B) a model including nitrogen limitation resulting from root senescence and the decrease of soil nitrogen concentration, (C) a model including a small nitrogen limitation and a large initial shoot–root ratio and (D) a model including a large nitrogen limitation and a large initial shoot–root ratio. The dashed line represents $y = x$. Crosses on the different trajectories represent root and shoot biomass at the harvesting dates, which are used to compute the allometric coefficient β. These various trajectories do not fit overall plant growth patterns, but are used here to illustrate the effects of the various model ingredients on root–shoot trajectories.

studied in Meziane and Shipley (1999). Thus three parameters remain to be to estimated in the minimal version of the model: A_{max}, a_N and U_{max}. Up to three additional parameters, ρ, K_m and R_0, need to be estimated in the additional versions of the model described above.

A $25 \times 26 \times 5 \times 7 \times 9 \times 19$ grid of parameter values was used (Table 3). The parameter space has been chosen so as to include the reported parameter values found in the literature (Table 3). In M_0, parameters ρ and K_m were set to zero. In models M_0 and M_1, initial shoot–root ratio R_0 was equal to the ratio predicted by optimal partitioning.

The same distance ε between model predictions and experimental data is used. This time, between four and six model parameters have to be estimated with only two growth indicators. Consequently, a large array of parameter sets can lead to model predictions matching the two growth indicators. Therefore, rather than trying to estimate the model parameters, the model simulations are filtered so that they fit the available growth indicators (Jabot and Bascompte, 2012). As previously, model parameter sets leading to ε values $<0{\cdot}05$ are retained. These retained realistic simulations are then used to explore the range of allometric relationships between root and shoot biomass that the three models are able to predict. To this end, for each model simulation, the same procedure as in Shipley and Meziane (2002) was used to compute the allometric coefficient β: plant biomass was simulated at 15, 20, 25, 30 and 35 d post-germination and β was computed as the slope of a regression of the natural logarithm of shoot dry mass on root dry mass. To quantify the predictive ability of the models, the relative distance between simulated and empirical values of allometric coefficients β is computed for every retained set of parameters, and the sets which lead to the smallest distance, called d_{min}, are kept:

$$d_{min} = \min\left(\sqrt{\left(\frac{(\beta_{obs} - \beta_{sim})^2}{(\beta_{obs})^2}\right)}\right) \quad (26)$$

where β_{obs} and β_{sim} are empirical and simulated values of the allometric coefficients.

Results

Model M_0 was found (as in the first section) to produce β values equal to 1 (Fig. 3A). Adding a decrease in root uptake efficiency with age and nitrogen consumption (model M_1) caused plants to become progressively limited in nitrogen and to allocate an increasing amount of biomass to roots as they grow. This led to β values <1 (Fig. 3B). When the initial shoot–root ratio was large, plants also allocated more biomass to roots until an optimal ratio was reached (model M_2). This also led to β values <1 (Fig. 3C), although it affected the beginning of the growth dynamics rather than the end as observed with nutrient limitation (Fig. 3B). These two processes were found to reinforce each other, since they acted at different growth stages (Fig. 3D).

The three models were fitted to the data of Shipley and Meziane (2002). Some models failed at reproducing some of the growth indicators with an average relative error $\varepsilon < 0{\cdot}05$. Model M_0 did not succeed in reproducing RGR and RWR of eight, 14, 18 and 21 out of the 22 species in the LN, lN, Ln and ln treatments, respectively (Fig. 4). When the effects of nitrogen limitation were included in the model (model M_1), the number of accurately reproduced growth patterns strongly increased: the growth indicators of 18, 20, 20 and 22 out of the 22 species could be reproduced in the lN, LN, Ln and ln treatments, respectively. The full model (M_2) was able to reproduce the growth indicators of all species accurately, except in the LN treatment (20 of the 22 species).

When models succeeded in reproducing the plant growth indicators, the allometric coefficients β that they predicted were compared with observed values. Model M_0 failed at reproducing such allometric coefficients, irrespective of the environmental

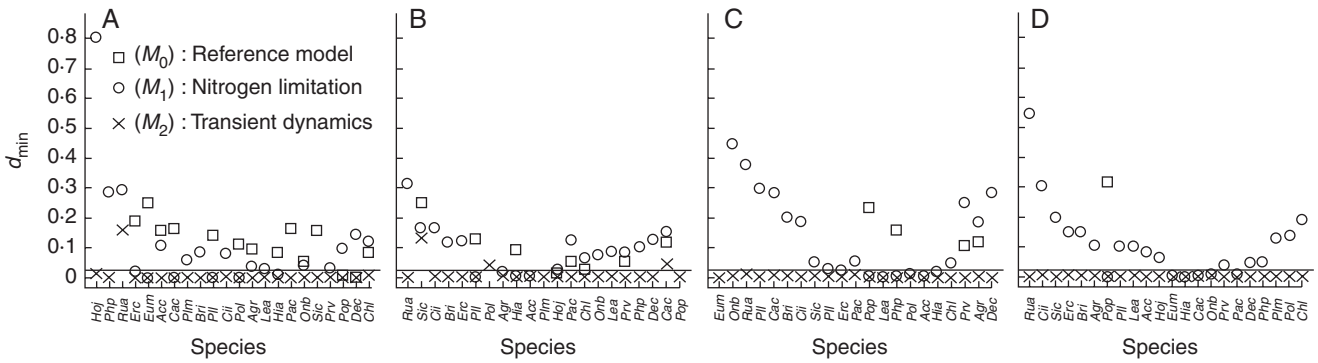

FIG. 4. Minimal relative distance d_{min} between empirical and simulated allometric coefficients β for each species studied in Shipley and Meziane (2002). (A) LN treatment. (B) lN treatment. (C) Ln treatment. (D) ln treatment. Species are sorted by increasing β values. Each symbol corresponds to a model. When a model did not succeed in reproducing growth indicators with a good accuracy, its corresponding point was not shown. The solid line represents a threshold d_{min} of 2·5 %. The abbreviations for species names used in the *x*-axis are detailed in Supplementary Data Table S1.

treatments. Adding nitrogen limitation weakly increased the predictive ability of the model: the relative distance d_{min} between empirical and simulated allometric coefficients was equal to zero for only seven species across all treatments, i.e. in 8 % of the cases. In contrast, model M_2 succeeded in reproducing observed allometric coefficients with d_{min} values almost always equal to zero, except for *Rumex acetosa* ($\beta = 0{\cdot}748$) in the LN treatment, *Deschampsia cespitosa* ($\beta = 1{\cdot}261$) in the Ln treatment and *Silene cucubalus* ($\beta = 0{\cdot}804$), *Polygonum lapathifolium* ($\beta = 0{\cdot}906$), *Plantago major* ($\beta = 0{\cdot}948$) and *Panicum capillare* ($\beta = 1{\cdot}000$) in the lN treatment (Fig. 4).

Even if a model fails at accurately predicting the empirical allometric coefficients, it may still make close predictions. β values simulated with model M_1 were closer to the empirical values of Shipley and Meziane (2002) than those simulated with model M_0 for all species with β values <1 (Fig. 4). The relative distance d_{min} between empirical and simulated β values was $>0{\cdot}10$ in 83 % of the cases for model M_0, while for model M_1, d_{min} was $<0{\cdot}025$ in 26 % of the cases and $<0{\cdot}10$ in 50 % of the cases. The full model (M_2) had relative errors d_{min} on β values $<0{\cdot}10$ for all species in all treatments, except for *R. acetosa* in the LN treatment.

Model validation

The modelling results make an additional prediction: in cases in which allometric coefficients β are significantly different from 1, this should be due to the difference between the initially constrained shoot–root ratio and the ratio required for optimal partitioning. If β is <1, the initial shoot–root ratio should be larger than the optimal ratio, and vice versa (Supplementary Data Fig. S1). This final prediction was tested by re-analysing the data of Shipley and Meziane (2002). The average initial shoot–root ratio and the standard deviation were computed from available biomass data, and a weighted least square regression was used to assess the accuracy of model predictions (Fig. 5).

For the LN and ln treatments, the initial shoot–root ratio predicted by the full model (M_2) fits the biomass raw data with a good accuracy ($r = 0{\cdot}87$ for the LN treatment and $r = 0{\cdot}53$ for the ln treatment). For the Ln and lN treatments, model predictions are not so good ($r = 0{\cdot}12$ for the lN treatment and $r = 0{\cdot}33$ for the Ln treatment). In these treatments, only five (respectively six) species out of 21 had a β value significantly different from 1 (Shipley and Meziane, 2002). When the regression was performed solely on species with an allometric coefficient significantly <1, the regression coefficient sharply increased to 0·80 for the lN treatment and to 0·63 for the Ln treatment. This means that model predictions regarding initial root–shoot ratios were close to observations in cases in which this ontogenetic constraint was necessary to explain root–shoot trajectories. In cases in which a simpler model was sufficient to account for observations, the uncertainty of the initial root–shoot ratio estimation obscured the predictions (Fig. 5).

DISCUSSION

This study aimed at testing whether observed root–shoot allometries during plant development could be explained by the hypothesis of optimal partitioning. The approach was thus 2-fold. First, a simple model of plant growth was built based on commonly measured plant functional traits, and then we tested whether this model was a sufficiently detailed account of plant growth to reproduce various growth indicators of experimental studies. The model succeeded in reproducing these indicators with a very good accuracy (Fig. 1). Two plant traits were not empirically measured during the experiments and were estimated to reproduce the two plant growth indicators. Fitted trait values were within the ranges reported in the literature, and were thus realistic. This first part of the study was essential to discard the possibility that the discrepancy between theoretical predictions and empirical allometries would be due to a poor modelled representation of plant growth.

The second part of the study aimed at using this simple model to predict root–shoot allometry during plant development. The results of previous simpler models were recovered: the optimal partitioning hypothesis led to an isometric growth of roots and shoot (Charles-Edwards *et al.*, 1972), in contrast to the empirical findings of Shipley and Meziane (2002). This steady-state isometry was further found to be preceded by a short transient period of non-isometric growth, during which plants were dynamically adjusting their allocation coefficient if initial root–shoot ratios were not optimal (Fig. 2). It was then tested whether adding complementary model ingredients could lengthen the duration of this transient phase and change the shape of the root–shoot

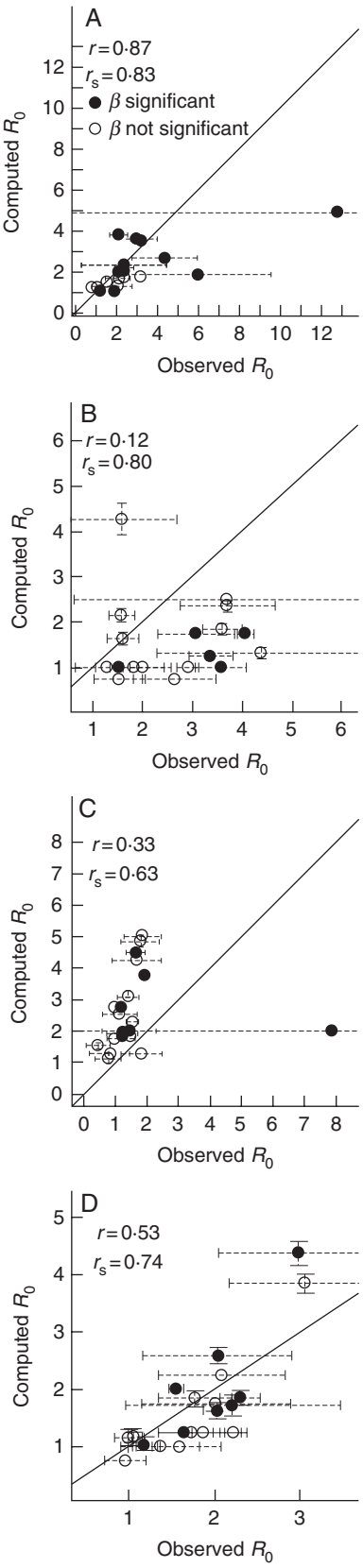

FIG. 5. Fitted initial shoot–root ratios against initial shoot–root ratios computed from the biomass raw data of Shipley and Meziane (2002) in (A) the LN treatment, (B) the lN treatment, (C) the Ln treatment and (D) the ln treatment. Each circle represents a species with β significantly or not significantly different from 1, as indicated in the key in (A). Standard deviations are drawn using dotted lines. Weighted least square regression coefficients were computed from all data (r) and from data with β significantly different from 1 (r_s).

allometry. Root senescence was added in the model, as well as the nitrogen consumption by plants in the experimental containers. These first two ingredients improved the ability of the models to reproduce growth indicators when light and nitrogen were limiting. However, they were insufficient to explain the results of Shipley and Meziane (2002) on allometric trajectories. The initial shoot–root ratio was then varied to represent initial developmental constraints. With this third ingredient, most of the empirical findings of Shipley and Meziane (2002) could be reproduced (Fig. 4).

These simulation results show that to be a reasonable approximation of the plant allocation scheme, the optimal partitioning framework needs to be complemented by a number of complementary processes which lead to transient phases of allocation adjustment by the plant. A combination of these processes was found to be necessary to recover the empirical findings of Shipley and Meziane (2002). More precisely, the initial shoot–root ratio had to be different from the ratio predicted by optimal partitioning to recover most of the allometric coefficients which were significantly different from 1. Gedroc *et al.* (1996) provided evidence that ontogenetic constraints were likely to play a role in allometric trajectories by statistically analysing plant growth trajectories. The modelling approach proposed here enabled us to incorporate mechanistically various processes that have been suggested in the literature to cause shifts in root–shoot scaling during plant ontogeny, and to test their respective influences quantitatively. Furthermore, this approach demonstrated that although adding some initial developmental constraints may be needed to recover experimental findings, such developmental constraints were no longer needed during the subsequent plant growth dynamics phase, which was controlled by optimal partitioning mechanisms.

The hypothesis that initial shoot–root ratios may differ from the ratio required for optimal partitioning is supported by the reanalysis of the experiments of Shipley and Meziane (2002) (Fig. 5). Moreover the finding that the initial shoot–root ratio should be larger than 1 during the very first days of plant growth after germination is consistent with observations (Jurado and Westoby, 1992; Leishman and Westoby, 1994). The hypothesis that this initial shoot–root ratio should be at least partially developmentally constrained is also consistent with observations (Evans, 1977; Kitajima, 2002) and the biological fact that initial plant growth is ensured by the consumption of seed reserves. The explanation modelled here for non-isometric root–shoot trajectories is hence uniquely based on transient dynamics controlled by optimal partitioning equations. The model proved powerful in the non-constant nutrient conditions of the experiments of Shipley and Meziane (2002) (when observed at an hourly resolution). This model could hence similarly be used to predict root–shoot dynamics quantitatively in response to disturbances (Mäkelä, 1999).

The model proposed here does not take into account self-shading, shoot senescence or water use by the plant. It is thus not able in its present form to assess potential explanations for

observed ontogenetic shifts in root–shoot scaling evidenced in longer term experiments (e.g. Mueller *et al*., 2000) for which these three effects could play an additional role. Similarly, it cannot be used in its present form to assess the potential role of temperature increase or water shortage in biomass allocation. Since these last two environmental pressures are likely to be important according to current climate change scenarios, further model refinements to add temperature and water effects constitute very interesting perspectives. Such future model developments will be facilitated by the general approach of progressive model building through quantitative assessment that has been developed in this study.

In this study, optimal allocation equations were based on the idea that the RGR should be a good proxy for plant fitness and thus should be optimized by evolution. However, plants have evolved in competitive environments, so that for a plant, maximizing its growth in isolation is not necessarily the best strategy to maximize its growth in competitive conditions (McNickle and Dybzinski, 2013). Future work addressing this issue would be valuable. Further studies would require the consideration of below-ground competition for soil resources and of above-ground competition for light (Tilman, 1988; Schieving and Poorter, 1999; Gersani *et al*., 2001; O'Brien and Brown, 2008). Such work would enable an understanding of whether the use of new plant fitness proxies in optimal partitioning modelling could also produce the long-lasting transient dynamics that have been evidenced here.

SUPPLEMENTARY DATA

Supplementary data are available online at www.aob.oxfordjournals.org and consist of the following. Table S1: list of abbreviations used for the species studied by Shipley and Meziane (2002). Figure S1: shoot–root ratio required for optimal partitioning and shoot–root ratio minimizing the distance between empirical and simulated allometric coefficients in the LN treatment, the Ln treatment., the lN treatment and the ln treatment.

ACKNOWLEDGEMENTS

T.L. was funded by the Institut national de Recherche en Sciences et Technologies pour l'Environnement et l'Agriculture (IRSTEA) and the region Auvergne.

LITERATURE CITED

Arredondo JT, Jones TA, Johnson DA. 1998. Seedling growth of Intermountain perennial and weedy annual grasses. *Journal of Range Management* **51**: 584–589.

Aschan G, Pfanz H. 2003. Non-foliar photosynthesis – a strategy of additional carbon acquisition. *Flora* **198**: 81–97.

Bloom A, Chapin F, Mooney H. 1985. Resource limitation in plants – an economic analogy. *Annual Review of Ecology and Systematics* **16**: 363–392.

Bonan G. 2008. Forests and climate change: forcings, feedbacks, and the climate benefits of forests. *Science* **320**: 1444–1449.

Brouwer R. 1962. Nutritive influences on the distribution of dry matter in the plant. *Netherlands Journal of Agricultural Science* **10**: 399–408.

Chapin F. 1980. The mineral nutrition of wild plants. *Annual Review of Ecology and Systematics* **11**: 233–260.

Charles-Edwards D. 1976. Shoot and root activities during steady-state plant growth. *Annals of Botany* **40**: 767–772.

Charles-Edwards D, Charles-Edwards J, Sant F. 1972. Models for mesophyll cell arrangement in leaves of ryegrass (lolium perenne l.). *Planta* **104**: 297–305.

Dewar R, Franklin O, Mäkelä A, McMurtrie R, Valentine H. 2009. Optimal function explains forest responses to global change. *BioScience* **59**: 127–139.

Dybzinski R, Farrior C, Wolf A, Reich P, Pacala S. 2011. Evolutionarily stable strategy carbon allocation to foliage, wood, and fine roots in trees competing for light and nitrogen: an analytically tractable, individual-based model and quantitative comparisons to data. *American Naturalist* **177**: 153–166.

Engels C, Neumann G, Gahoonia TS, George E, Schenk MK. 2000. Assessing the ability of roots for nutrients acquisition. In: Smit AL, Bengough AG, Engels C, van Noordwijk M, Pellerin S, van de Geijn S, eds. *Root methods. A handbook*. Berlin: Springer, 403–459.

Evans G. 1972. *The quantitative analysis of plant growth*. University of California Press.

Evans PS. 1977. Comparative root morphology of some pasture grasses and clovers. *New Zeland Journal of Agricultural Research* **20**: 331–335.

Foley J. 2007. Net primary productivity in the terrestrial biosphere: the application of a global model. *New Phytologist* **174**: 811–822.

Franklin O, Johansson J, Dewar R, *et al*. 2012. Modeling carbon allocation in trees: a search for principles. *Tree Physiology* **32**: 648–666.

Gedroc J, McConnaughay K, Coleman J. 1996. Plasticity in root/shoot partitioning: optimal, ontogenetic, or both? *Functional Ecology* **10**: 44–50.

Gersani M, Bown J, O'Brien E, Maina G, Abramsky Z. 2001. Tragedy of the commons as a result of root competition. *Journal of Ecology* **89**: 660–669.

Goudriaan J, Van Laar H. 1994. *Modelling potential crop growth processes*. Dordrecht, The Netherlands: Kluwer Academic Publishers.

Grime JP. 2001. *Plant strategies, vegetation processes, and ecosystem properties*, 2nd. edn. Chichester, UK: Wiley.

Génard M, Dauzat J, Franck N, *et al*. 2008. Carbon allocation in fruit trees: from theory to modelling. *Trees* **22**: 269–282.

Hungate B, Holland E, Jackson R, Chapin F, Mooney H. 1997. On the fate of carbon in grasslands under carbon dioxide enrichment. *Nature* **579**: 388–576.

Ingestad T, Ågren GI. 1991. The influence of plant nutrition on biomass allocation. *Ecological Applications* **1**: 168–174.

Iwasa Y, Roughgarden J. 1984. Shoot/root balance of plants: optimal growth of a system with many vegetative organs. *Theoretical Population Biology* **25**: 78–105.

Jabot F, Bascompte J. 2012. Bitrophic interactions shape biodiversity in space. *Proceedings of the National Academy of Sciences USA* **109**: 4521–4526.

Johnson IR. 1985. A model of partitioning of growth between the shoots and roots of vegetative plants. *Annals of Botany* **55**: 421–431.

Johnson IR, Thornley JHM. 1987. A model of shoot:root partitioning with optimal growth. *Annals of Botany* **60**: 133–142.

Jurado E, Wetoby M. 1992. Seedling growth in relation to seed size among species of arid Australia. *Journal of Ecology* **80**: 407–416.

Kattge J, Diaz S, Lavorel S, *et al*. 2011. Try – a global database of plant traits. *Global Change Biology* **17**: 2905–2935.

Kikuzawa K, Lechowicz M. 2006. Toward synthesis of relationships among leaf longevity, instantaneous photosynthetic rate, lifetime leaf carbon gain, and the gross primary production of forests. *American Naturalist* **168**: 373–383.

Kitajima K. 2002. Do shade-tolerant tropical tree seedlings depend longer on seed reserves? Functional growth analysis of three Bignoniaceae species. *Functional Ecology* **16**: 433–444.

Konings H, Koot E, De Wolf A. 1989. Growth characteristics, nutrient allocation and photosynthesis of carex species from floating fens. *Oecologia* **80**: 111–121.

Lambers H, Chapin F, Pons T. 1998. *Plant physiological ecology*. New York: Springer-Verlag.

Leishman M.R., Westoby M. 1994. The role of large seed size in shaded conditions: experimental evidence. *Functional Ecology* **8**: 205–214.

Le Roux X, Lacointe A, Escobar-Gutiérrez A, Le Dizes S. 2001. Carbon-based models of individual tree growth: a critical appraisal. *Annals of Forest Science* **58**: 469–506.

Maire V, Gross N, Da Silveira Pontes L, Picon-Cochard C, Soussana J. 2009. Trade-off between root nitrogen acquisition and shoot nitrogen utilization across 13 co-occurring pasture grass species. *Functional Ecology* **23**: 668–679.

Mäkelä A, Valentine H, Helmisaari H. 2008. Optimal co-allocation of carbon and nitrogen in a forest stand at steady state. *New Phytologist* **180**: 114–123.

Mäkelä A. 1999. Acclimatation in dynamic models based on structural relationships. *Functional Ecology* **13**: 145–156.
McConnaughay KDM, Coleman JS. 1999. Biomass allocation in plant: ontogeny or optimality? A test along three resource gradients. *Ecology* **80**: 2581–2593.
McNickle G, Dybzinski R. 2013. Game theory and plant ecology. *Ecology Letters* **16**: 545–555.
Meziane D, Shipley B. 1999. Interacting components of interspecific relative growth rate: constancy and change under differing conditions of light and nutrient supply. *Functional Ecology* **13**: 311–622.
Mokany K, Raison R, Prokushkin A. 2006. Critical analysis of root:shoot ratios in terrestrial biomes. *Global Change* **12**: 84–96.
Morris JT. 1980. The nitrogen uptake kinetics of *Spartina alterniflora* in culture. *Ecology* **61**: 1114–1121.
Müller I, Schmid B, Weiner J. 2000. The effect of nutrient availability on biomass allocation patterns in 27 species of herbaceous plants. *Perspectives in Plant Ecology, Evolution and Systematics* **3**: 115–127.
Niklas K. 1994. *Plant allometry. The scaling of form and process*. Chicago University Press.
Nilsen E. 1995. Stem photosynthesis: extent, patterns, and role in plant carbon economy. In: Gartner BL, ed. *Plant stems: physiology and functional morphology*. New York: Academic Press, 223–256.
O'Brien E, Brown J. 2008. Games roots play: effects of soil volume and nutrients. *Journal of Ecology* **96**: 438–446.
Poorter H, Niklas K, Reich P, Oleksyn J, Poot P, Mommer L. 2012. Biomass allocation to leaves, stems and roots: meta-analyses of interspecific variation and environmental control. *New Phytologist* **193**: 30–50.
Reich PB, Buschena C, Tjoelker M, *et al.* 2003. Variation in growth rate and ecophysiology among 34 grassland and savannah species under contrasting N supply: a test of functional group differences. *New Phytologist* **157**: 617–631.
Reynolds JF, Thornley JHM. 1982. A shoot:root partitioning model. *Annals of Botany* **49**: 585–597.
Reynolds J, Chen J. 1996. Modeling whole-plant allocation in relation to carbon and nitrogen supply: coordination versus optimization. *Plant and Soil* **185**: 65–74.
Robinson D. 1986. Limits to nutrient inflow rates in roots and root systems. *New Phytologist* **68**: 551–559.
Schieving F, Poorter H. 1999. Carbon gain in a multispecies canopy: the role of specific leaf area and photosynthetic nitrogen-use efficiency in the tragedy of the commons. *New Phytologist* **143**: 201–211.
Schippers P, Kropff MJ. 2001. Competition for light and nitrogen among grassland species: a simulation analysis. *Functional Ecology* **15**: 155–164.
Shipley B, Meziane D. 2002. The balanced-growth hypothesis and the allometry of leaf and root biomass allocation. *Functional Ecology* **16**: 326–331.
Taubert F, Frank K, Huth A. 2012. A review of grassland models in the biofuel context. *Ecological Modelling* **245**: 84–93.
Thornley J. 1995. Shoot:root allocation with respect to C, N and P: an investigation and comparison of resistance and teleonomic models. *Annals of Botany* **75**: 391–405.
Thornley J. 1998. *Grassland dynamics: an ecosystem simulation model*. Wallingford, UK: CAB International.
Tilman D. 1988. *Plant strategies and the dynamics and structure of plant communities*. Princeton University Press.
Tucker MR. 1999. *Clay minerals: their importance and function in soils. Soil Fertility Note 13, NCDA&CS Agronomic Division*. Downloadable at www.ncagr.gov/agronomi/pdffiles/sfn13.pdf.
Valentine HT, Mäkelä A. 2012. Modeling forest stand dynamics from optimal balances of carbon and nitrogen. *New Phytologist* **194**: 961–971.
Volder A, Smart D, Bloom A, Eissenstat D. 2005. Rapid decline in nitrate uptake and respiration with age in fine lateral roots of grape: implications for root efficiency and competitive effectiveness. *New Phytologist* **165**: 493–502.
West G, Brown J, Enquist B. 1999. The fourth dimension of life: fractal geometry and allometric scaling of organisms. *Science* **284**: 1677–1679.

SUPPLEMENTARY DATA

TABLE S1. List of abbreviations used for the species studied by Shipley and Meziane (2002).

Abbreviation	Species
Acc	*Acorus calamus*
Agr	*Agropyron repens*
Bri	*Bromus inermis*
Cac	*Carex crinita*
Chl	*Chrysanthemum leucanthemumu*
Cii	*Cichorium intybus*
Dec	*Deschampsia cespitosa*
Erc	*Erysimum cheirantoides*
Eum	*Eupatorium maculatum*
Hia	*Hieracium aurantiacum*
Hoj	*Hordeum jubatum*
Lea	*Leontodon autumnalis*
Onb	*Oenothera biennis*
Pac	*Panicum capillare*
Php	*Phleum pratense*
Pll	*Plantago lanceolata*
Plm	*Plantago major*
Pop	*Poa pratensis*
Pol	*Polygonum lapathifolium*
Prv	*Prunella vulgaris*
Rua	*Rumex acetosa*
Sic	*Silene cucubalus*

FIG. S1. Shoot-root ratio required for optimal partitioning (+) and shoot-root ratio minimizing the distance between empirical and simulated allometric coefficients (○) in (A) the LN treatment,. (B) the Ln treatment., (C) the lN treatment, and (D) the ln treatment. Species are sorted by increasing β values. The abbreviations for species names used in the *x*-axis are detailed in Table S1.